Brf1 posttranscriptionally regulates pluripotency and differentiation responses downstream of Erk MAP kinase

Frederick E. Tan[a,b] and Michael B. Elowitz[a,b,1]

[a]Howard Hughes Medical Institute and [b]Division of Biology and Departments of Bioengineering and Applied Physics, California Institute of Technology, Pasadena, CA 91125

Edited by Gideon Dreyfuss, University of Pennsylvania, Philadelphia, PA, and approved March 25, 2014 (received for review November 6, 2013)

AU-rich element mRNA-binding proteins (AUBPs) are key regulators of development, but how they are controlled and what functional roles they play depends on cellular context. Here, we show that Brf1 (*zfp36l1*), an AUBP from the Zfp36 protein family, operates downstream of FGF/Erk MAP kinase signaling to regulate pluripotency and cell fate decision making in mouse embryonic stem cells (mESCs). FGF/Erk MAP kinase signaling up-regulates Brf1, which disrupts the expression of core pluripotency-associated genes and attenuates mESC self-renewal without inducing differentiation. These regulatory effects are mediated by rapid and direct destabilization of Brf1 targets, such as Nanog mRNA. Enhancing Brf1 expression does not compromise mESC pluripotency but does preferentially regulate mesendoderm commitment during differentiation, accelerating the expression of primitive streak markers. Together, these studies demonstrate that FGF signals use targeted mRNA degradation by Brf1 to enable rapid posttranscriptional control of gene expression in mESCs.

stem cell biology | AU-rich element RNA-binding proteins | developmental mechanisms | developmental signaling pathways | gene regulation dynamics

AU-rich element mRNA-binding proteins (AUBPs) represent an important class of regulators required for the proper development of embryonic and adult tissues in the mouse (1), but whether they have developmentally important roles in mouse embryonic stem cells (mESCs) remains unclear. A recent proteomic survey identified more than 500 mRNA-binding proteins in mESCs, several of which are AUBPs (2). Independent of the micro-RNA pathway, AUBPs are known regulators of splicing, mRNA stability, translational efficiency, and RNA transport (3), and could provide an additional layer of developmental regulation that complements other pluripotency and self-renewal mechanisms. AUBPs are essential in many developmental systems, such as during hematopoiesis, neurogenesis, germ cell commitment, and placental morphogenesis (4–6). Their absence or misregulation can be lethal and often promotes disease progression (7–9). Despite growing interest in the many functions of AUBPs, their regulation and function in mESCs remains poorly understood.

The expression and activity of AUBPs is known to be regulated by growth factor signaling in many cellular contexts (10, 11). In mESCs, the FGF/Erk MAP kinase signaling pathway is a central regulator of self-renewal, pluripotency, and differentiation (12, 13). Although much is known about the developmental effects of FGF/Erk MAP kinase signaling inhibition or activation (14, 15), the regulatory mechanisms used downstream of Erk1/2 often remain unclear. Various transcriptional, posttranscriptional, and posttranslational mechanisms are engaged to regulate target genes (16). As part of this signaling cascade, AUBPs could mediate rapid signaling-dependent responses, but this potential role has not been investigated.

Here, we show that the expression of Brf1 (*zfp36l1*) is regulated by FGF/Erk MAP kinase signaling in both pluripotent and differentiating mESCs. Brf1 is a member of the Zfp36 AUBP family that plays critical roles throughout mouse development. Without Brf1, embryos die in utero at approximately embryonic day 10.5 (E10.5) as a result of allantoic, placental, and neural tube defects (9), and its absence in adults promotes leukemia (17). In mESCs, Brf1 binds AU-rich sequences in many pluripotency-associated mRNAs, including Nanog, to regulate their localization and abundance. This regulation broadly perturbs the core transcription factor network without inducing differentiation, but compromises the capacity to self-renew. In differentiation-stimulating conditions, Brf1 enhances the expression of primitive streak markers, indicating an accelerated commitment to mesendoderm. Together, these data identify targeted mRNA degradation by Brf1 as a mechanism through which the biology of mESCs is regulated and controlled by FGF/Erk MAP kinase signals.

Results

Erk MAP Kinase Signaling Regulates the Expression of Zfp36 AUBPs. AUBP expression in mESCs has been documented by several groups (2, 9, 18). The known sensitivity of AUBPs to growth factors suggested that these proteins could be regulated by FGF/Erk MAP kinase signaling (11, 19). To explore this potential regulatory connection, we first profiled the transcriptome of E14 mESCs using high-throughput sequencing to determine which AUBPs are actively expressed (Fig. 1*A* and Dataset S1). We identified several classes of AUBPs, including (*i*) members of the

Significance

Intercellular signaling pathways strongly regulate gene expression in uncommitted precursor stem cells, but the mechanisms through which these signaling pathways regulate gene targets often remain unclear. We address this question in mouse embryonic stem cells (mESCs) and highlight the importance of AU-rich element mRNA-binding proteins as regulatory intermediates of intercellular signaling. We show that the FGF/Erk MAP kinase signaling pathway strongly influences the expression of Brf1, a member of the Zfp36 protein family that is known to bind and destabilize its mRNA targets. Brf1 physically binds many pluripotency and differentiation-associated mRNAs. Moderate changes in its expression compromise self-renewal capacity and bias fate commitment, thus providing a posttranscriptional link between intercellular signaling activity and gene expression in mESCs.

Author contributions: F.E.T. and M.B.E. designed research; F.E.T. performed research; F.E.T. contributed new reagents/analytic tools; F.E.T. and M.B.E. analyzed data; and F.E.T. and M.B.E. wrote the paper.

The authors declare no conflict of interest.

This article is a PNAS Direct Submission.

Data deposition: The data reported in this paper have been deposited in the Gene Expression Omnibus (GEO) database, www.ncbi.nlm.nih.gov/geo (accession no. GSE40104).

[1]To whom correspondence should be addressed. E-mail: melowitz@caltech.edu.

This article contains supporting information online at www.pnas.org/lookup/suppl/doi:10.1073/pnas.1320873111/-/DCSupplemental.

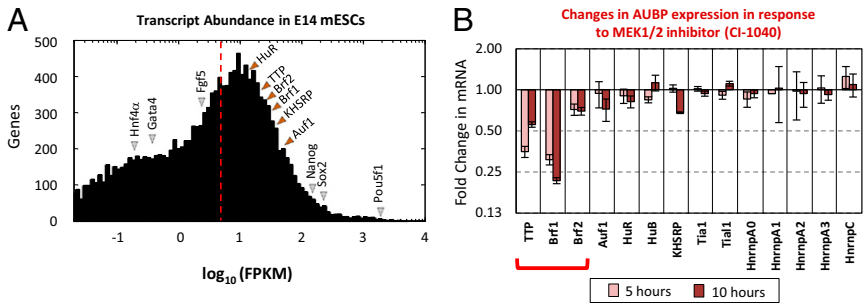

Fig. 1. Erk MAP kinase signaling regulates AUBP expression in mESCs. (*A*) Distribution of average transcript abundances (FPKM) from two total RNA biological replicates. Highlighted are notable mESC pluripotency and differentiation genes (gray triangles), which were used to distinguish actively expressed genes (mean FPKM ≥ 5, 7,194 genes) from the gene expression background (mean FPKM < 5, 11,119 genes). FPKM = 5 denoted by red dashed line. Well-characterized and actively expressed AUPBs are highlighted (orange triangles). (*B*) Profiling changes in AUBP expression using RT-qPCR in response to a pharmacological inhibitor of MEK1/2 (CI-1040/PD184352) after 5 and 10 h. Members of the Zfp36 family are highlighted in the red bracket.

Zfp36 protein family [TTP (*zfp36*), Brf1 (*zfp36l1*), and Brf2 (*zfp36l2*)], which are known to play critical roles during hematopoiesis by destabilizing Cytokine and Notch-Delta signaling-associated mRNAs; (*ii*) members of the Hu protein family [HuR (*elavl1*), HuB (*elavl2*)], which stabilize their mRNA targets and are known to actively regulate germ cell development; and (*iii*) Auf1 (*hnrnpd*), which can stabilize or destabilize mRNA and modulate inflammation in the adult mouse (20).

To determine whether any of the detected AUBPs was regulated by FGF/Erk MAP kinase signaling, we measured changes in their expression in response to pharmacological inhibitors of MEK1/2. We discovered that TTP and Brf1 responded strongly to MEK1/2 inhibition, with mRNA levels down-regulated greater than twofold after 5 and 10 h (Fig. 1*B*). Brf2, Auf1, and KHSRP mRNA levels were also slightly down-regulated. Interestingly, three out of five of these responding genes are members of the Zfp36 protein family (Fig. 1*B*, red bracket).

Changes in Erk MAP Kinase Signaling Lead to Transient and Sustained Zfp36 Responses. We explored the regulatory connection between Zfp36 AUBPs and FGF/Erk MAP kinase signaling further by measuring how TTP, Brf1, and Brf2 responded to short and long periods of MEK1/2 inhibition (Fig. 2*A*). Incubation with MEK1/2 inhibitor resulted in a rapid reduction in TTP, Brf1, and Brf2

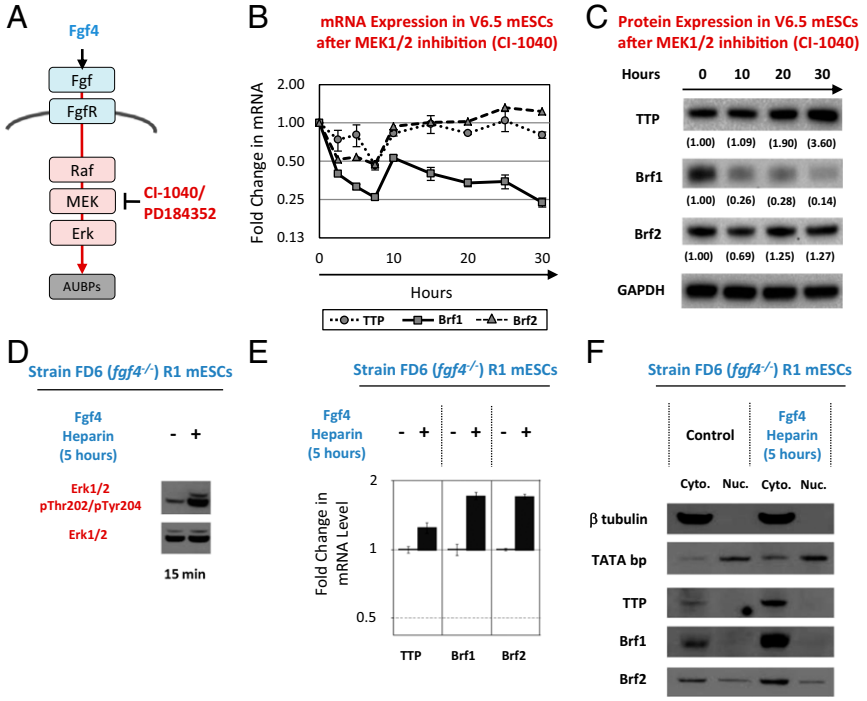

Fig. 2. FGF/Erk MAP kinase signaling regulates the expression of Zfp36 RBPs. (*A*) Cartoon depicting the potential relationship between FGF/Erk MAP kinase signaling and AUBP expression. Whereas the addition of Fgf4/heparin activates the FGF/Erk MAP kinase pathway, culturing cells with 5 μM PD184352/CI-1040 inhibits Erk1/2 activation. (*B*) A 30-h RT-qPCR time course of TTP, Brf1, and Brf2 mRNA level changes in response to MEK1/2 pharmacological inhibitors (±SEM; $n = 3$ for all time points), and (*C*) corresponding Western blots. (*D*) Western blot staining for Erk1/2 and phospho-Erk1/2 (Thr202/Tyr204) showing pathway activation in cells stimulated with 10 ng/mL FGF4 plus 10 μg/mL heparin for 15 min. (*E*) Changes in TTP, Brf1, and Brf2 after 5-h incubation with or without FGF4/heparin as indicated (±SEM; $n = 3$). (*F*) Western blot profiling of changes in TTP, Brf1, and Brf2 protein level in *fgf4*$^{-/-}$ mESCs after stimulation with FGF4/heparin for 5 h. To compare changes in intracellular localization, proteins were harvested sequentially as cytoplasmic (cyto) or nuclear (nuc) fractions, with β-tubulin and TATA-binding protein serving as localization controls. Also see Fig. S1 *A–D*.

mRNA level as gauged by reverse transcription–quantitative PCR (RT-qPCR) (Fig. 2*B*). Brf1, Brf2, and, to a lesser extent, TTP mRNA level changes were significant within 1 h of inhibitor treatment (Fig. S1*A*) and continued to decrease after 7.5 h of inhibition (Fig. 2*B*). However, after 10 h, TTP and Brf2 mRNA expression recovered, whereas Brf1 expression remained suppressed (Fig. 2*B*). Because the pharmacological inhibitor provides continuous suppression of Erk MAP kinase signaling (Fig. 2 and Fig. S1*B*), these data indicate that TTP and Brf2 mRNA respond only transiently (t < 10 h) to changes in Erk MAP kinase signaling, whereas Brf1 mRNA maintains a sustained response to the level of Erk MAP kinase signaling.

Protein level changes were also rapid, with a 30% reduction in TTP and a 50% reduction in Brf1 within 1.5 h of inhibitor treatment (Fig. 2 and Fig. S1*C*). However, whereas Brf1 protein levels continued to fall for the remainder of the time course, reaching ∼10-fold less protein by 30 h, TTP protein levels recovered and increased above DMSO-treated controls (Fig. 2*C*). These data indicate that the regulation of TTP protein becomes distinct from the regulation of TTP mRNA at later times (compare Fig. 2 *B* and *C*). We note that, in other cellular contexts, direct phosphorylation of TTP protein by Erk1/2 has been shown to reduce its stability (10). Furthermore, Zfp36 AUBPs also contain AU-rich sequences in their own mRNAs, which enable direct autoregulation and cross-regulation (Fig. 2 and Fig. S1*D*). These mechanisms could explain why TTP protein and mRNA levels respond differently after prolonged MEK1/2 inhibition. In contrast, Brf2 protein levels were much less affected, dropping slightly at 10 h, and then recovering at later time points. Thus, at both the mRNA and protein levels, Brf2

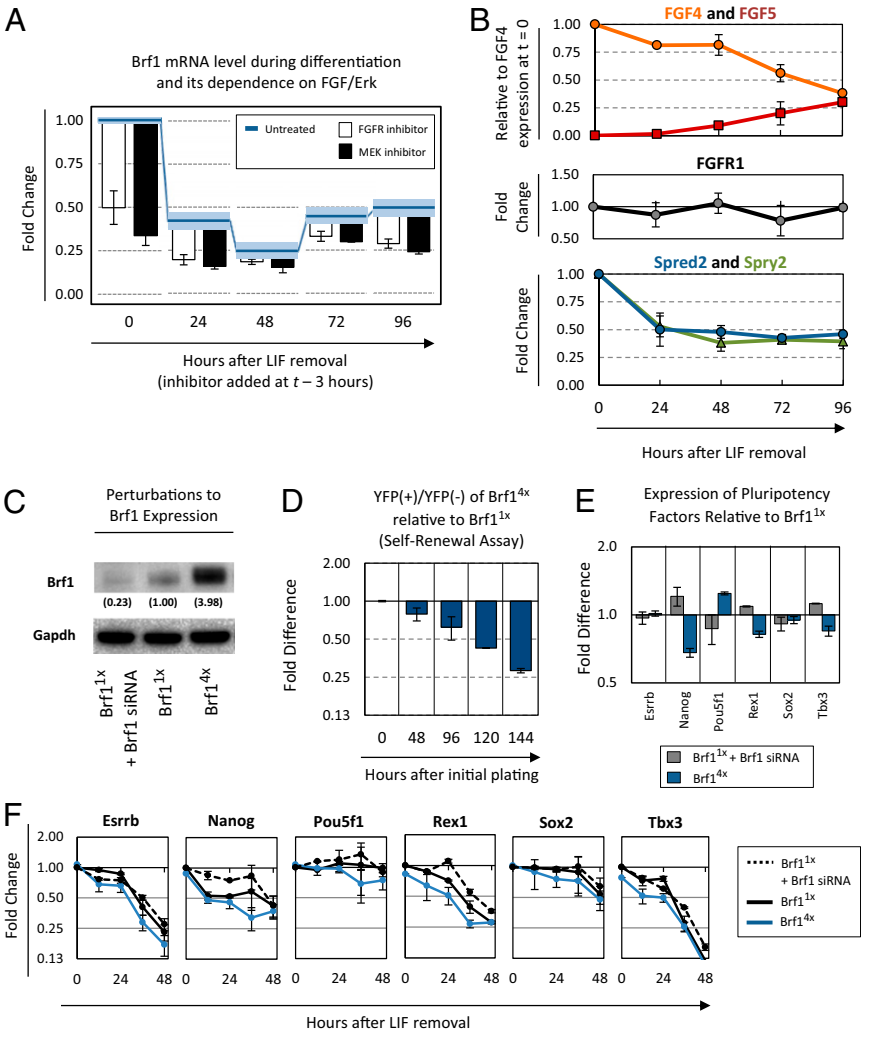

Fig. 3. Brf1 expression compromises mESC self-renewal. (*A*) Changes in Brf1 expression after LIF removal (blue line; light blue bounding boxes at each time point represent ±SEM; $n = 3$). The effect of FGF or Erk MAP kinase signaling inhibition on Brf1 expression at each time point is indicated (white and black bars, resulting from a 3-h inhibitor treatment) (±SEM; $n = 3$). (*B*) Changes in FGF4, FGF5, FGFR1, Spred2, and Spry2 mRNA expression after LIF removal (±SD; $n = 2$). (*C*) Brf1 expression was profiled in E14 carrying a CMV-H2B-YFP expression cassette (Brf1$^{1\times}$), Brf1$^{1\times}$ treated with Brf1 siRNAs, and E14 carrying a CMV-Brf1/T2A/H2B-YFP expression cassette (Brf1$^{4\times}$). A Western blot of Brf1 protein shows that siRNA knockdown reduced Brf1 expression by 75% after 36 h, and stable CMV-driven Brf1 expression increases Brf1 protein levels by fourfold relative to Brf1$^{1\times}$. Chemiluminescent intensities were normalized to Gapdh signal as loading control. (*D*) Changes in self-renewal of Brf1$^{4\times}$ relative to Brf1$^{1\times}$. Differences in proliferation rate were gauged by changes in the ratio of YFP(+) transgene-expressing cells to YFP(−) wild-type cells. For $t = 48$ and 96 h (±SEM; $n = 4$). For $t = 120$ and 144 h (±SEM; $n = 3$). (*E*) Changes in the expression of core pluripotency genes via RT-qPCR after Brf1 siRNA knockdown in Brf1$^{1\times}$ (gray bars) or enhanced Brf1 expression in Brf1$^{4\times}$ (blue bars) over 36 h (±SEM; $n = 2$). (*F*) Profiling changes in the expression of core pluripotency genes via RT-qPCR during the early stages of differentiation (15% serum, without LIF) in Brf1$^{1\times}$ treated with Brf1 siRNAs (dashed black line), Brf1$^{1\times}$ (solid black line), and Brf1$^{4\times}$ (solid blue line) (±SEM; $n = 2$).

responds more weakly to these perturbations (compare Fig. 2 *B* and *C*). These results indicate that AUBP levels respond to changes in Erk MAP kinase signaling with different kinetics.

To further validate these findings, we checked whether up-regulating FGF signaling could produce opposite results to inhibition (Fig. 2*A*). We added FGF4/heparin to *fgf4*$^{-/-}$ R1 mESCs (strain FD6), to activate Erk MAP kinase signaling (Fig. 2*D*) (21). TTP, Brf1, and Brf2 mRNA levels increased within 5 h of ligand addition, with similar changes at the protein level (Fig. 2 *E* and *F*). These changes occurred specifically within the cytoplasmic compartment, consistent with a role for these AUBPs in regulating targeted degradation of mature mRNAs (Fig. 2*F*). Together, these results indicate Zfp36 protein expression responds rapidly to both increases and decreases in FGF/Erk MAP kinase signaling activity, leading to both transient (TTP, Brf2) and sustained (Brf1) regulatory responses.

Enhancing Brf1 Compromises mESC Self-Renewal. Among the Zfp36 AUBPs, FGF/Erk MAP kinase signaling most strongly regulated the expression of Brf1 in pluripotent conditions (Fig. 2). During differentiation, Brf1 regulation was also dynamic and continued to be regulated by FGF/Erk MAP kinase signaling (Fig. 3*A*). The approximately twofold reduction in Brf1 expression over 4 d of LIF withdrawal (Fig. 3*A*) tracked concomitant changes in FGF4 expression (Fig. 3*B*), and the down-regulation of the Erk MAP kinase target genes Spred2 and Spry2 (Fig. 3*B*).

To determine the functional effect of Brf1 on pluripotent and differentiating cells, we perturbed Brf1 expression using siRNAs, which produced an approximately fourfold decrease in Brf1 protein relative to wild type. We also created stable transgene-mediated overexpression cell lines, which increased Brf1 protein levels approximately fourfold above wild-type levels (Fig. 3*C*). For transgene expression in mESCs, clones expressing H2B-YFP (Brf1$^{1\times}$) or Brf1-T2A-H2B-YFP (Brf1$^{4\times}$) were derived for these studies. Of these, one control Brf1$^{1\times}$ clone that expressed wild-type levels of Brf1 protein, and one Brf1$^{4\times}$ clone expressing approximately fourfold more Brf1 protein, was chosen for further analysis.

To quantify changes in mESC self-renewal brought about by Brf1 overexpression, we cocultured YFP(+) Brf1$^{4\times}$ clones with wild-type YFP(−) E14 mESCs. In this assay, any change in self-renewal ability manifests as changes in relative proliferation rate, and hence, a change in the YFP(+)/YFP(−) ratio (22). Compared with Brf1$^{1\times}$, cocultures with Brf1$^{4\times}$ exhibited a significant proliferation defect, with the YFP(+)/YFP(−) ratio reduced by ~20% every 48 h (Fig. 3*D*). In these cells, the expression of several core pluripotency genes is altered (Fig. 3*E*). However, most remain pluripotent in conditions with LIF plus serum (see below). Removing LIF rapidly initiates differentiation, and during the first 48 h, Brf1 siRNA knockdown in Brf1$^{1\times}$ or Brf1 overexpression in Brf1$^{4\times}$ produced only modest effects on the rate at which some markers of pluripotency were down-regulated (Fig. 3*F*).

Enhancing Brf1 Expression Accelerates Mesendoderm Differentiation. In contrast to the mild effect of Brf1 expression on the down-regulation of pluripotency factors (Fig. 3*F*), the up-regulation of

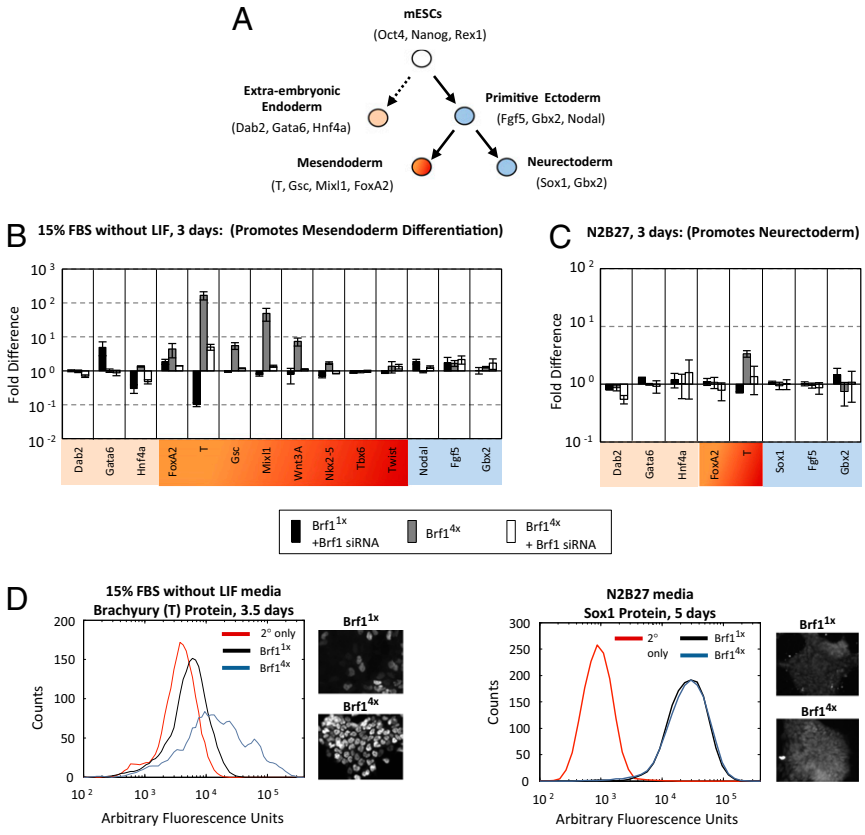

Fig. 4. Brf1 expression promotes mesendoderm differentiation. (*A*) Cartoon diagram showing the developmental potential of mESCs and associated lineage-specific markers. (*B*) Brf1$^{1\times}$ and Brf1$^{4\times}$ were cultured in mesoderm differentiation media (15% serum without LIF) for 3 d. Fold difference in the expression of several lineage-specific differentiation markers in Brf1$^{4\times}$ relative to Brf1$^{1\times}$ after 3 d of differentiation (±SEM; $n = 3$). (*C*) Brf1$^{1\times}$ and Brf1$^{4\times}$ were cultured in neurectoderm differentiation media (N2B27) for 3 d. Fold difference in the expression of several lineage-specific differentiation markers in CMV-Brf1 E14 relative to control E14 after 3 d of differentiation (±SEM; $n = 3$). (*D*) (*Left*) Brachyury immunostain and associated flow cytometry data after 3.5 d of differentiation ($n = 2{,}000$ cells). (*Right*) Sox1 immunostain and associated flow cytometry data after 5 d of differentiation ($n = 1{,}500$ cells).

differentiation markers is strongly affected by Brf1 (Fig. 4*A*). After 3 d of LIF withdrawal, we observed a striking bias in gene expression when comparing $Brf1^{4\times}$ to $Brf1^{1\times}$ cultures. LIF withdrawal generally promotes mesoderm differentiation (23). Indeed, Brachyury (T) was up-regulated in differentiating $Brf1^{1\times}$ and $Brf1^{4\times}$ cultures. However, Brachyury expression was 100-fold greater in the $Brf1^{4\times}$ cell line (Fig. 4*B*). Transfecting $Brf1^{1\times}$ cultures with Brf1 siRNAs produced the opposite effect, down-regulating Brachyury expression approximately fourfold relative to untreated controls (Fig. 4*B*). Furthermore, siRNAs against Brf1 could attenuate the up-regulation of Brachyury in $Brf1^{4\times}$, indicating that this regulation resulted specifically from Brf1 overexpression. In agreement with these results, flow cytometry profiling indicated that a larger fraction of $Brf1^{4\times}$ cells expressed Brachyury protein by 84 h compared with $Brf1^{1\times}$ (Fig. 4*D*). These findings were further supported by the up-regulation of mesendodermal markers Goosecoid (Gsc), Mixl1, and Wnt3A (Fig. 4*B*), indicating that Brf1 accelerated commitment to mesendodermal fates. Ectoderm markers (Nodal, Fgf5, and Gbx) were not affected, whereas extraembryonic and definitive endoderm markers (Gata6, Hnf4a, and FoxA2) showed weaker basal expression levels that responded differentially to Brf1 (Fig. 4*B*).

Brf1 expression did not influence neural differentiation. Because serum inhibits neural differentiation (24), we cultured cells in N2B27 serum-free media without LIF and BMP4. After 3 d in this media, most markers of differentiation appeared to be unaffected by Brf1 (Fig. 4*C*). For example, Sox1 mRNA and protein were readily detected, but its expression levels were similar in $Brf1^{1\times}$ and $Brf1^{4\times}$ cultures (Fig. 4 *C* and *D*). Interestingly, even in N2B27, the basal expression of Brachyury was up-regulated in a Brf1-dependent manner. Thus, Brf1 appears to mainly affect mesendodermal differentiation pathways.

Brf1 Binds Pluripotency-Associated mRNAs. To better understand the mechanistic basis for these developmental effects, we profiled possible Brf1 mRNA targets in mESCs. To determine which actively expressed genes are bound by Brf1, we adapted a previously developed RNA immunoprecipitation sequencing-based (RIPseq) assay that could selectively enrich target mRNAs using an affinity-purified polyclonal antibody against Brf1 (Fig. 5*A*; *Materials and Methods*) (25). In parallel, we performed a negative control using a nonspecific rabbit IgG. RNA from samples and controls were then processed and analyzed using high-throughput sequencing.

To provide a quantitative measure of antibody-mediated enrichment, we computed a statistic, denoted E_{RIP} for each actively expressed transcript (*Materials and Methods*). E_{RIP} represents the amount of mRNA coprecipitated with Brf1 protein over nonspecific background levels (*Materials and Methods*). Genes with high E_{RIP} values were more likely to have AU-rich elements (AREs) in their 3′-UTR (Fig. 5*B*). For example, considering the transcripts most enriched by Brf1 immunoprecipitation (positive outliers, $E_{RIP} > 1.226$, 418 genes), 25.1% contained the minimal full consensus ARE and 60.0% contained the minimal partial consensus ARE. These percentages represent a threefold to fourfold increase in ARE abundance relative to their frequency among all protein coding genes (Table S1 and Datasets S2–S4). Moreover, several of the most highly enriched target genes were previously characterized as direct targets of Zfp36 proteins (e.g., Ier3, Mllt11, and Pim3), including Zfp36 proteins themselves (26, 27). Interestingly, based on our definition of the minimal ARE element, many highly enriched target genes do not contain consensus AREs. However, the existence of noncanonical (although still poorly characterized) AU-rich sequences has been documented and could explain the enrichment of these mRNAs (28). Thus, the RIPseq assay can selectively enrich for mRNAs containing AREs.

Several pluripotency-associated factors were detected in the Brf1-RIP fraction, potentially explaining the developmental effects of Brf1 overexpression. For example, the core pluripotency regulators Nanog ($E_{RIP} = 0.58$) and Klf2 ($E_{RIP} = 7.15$) were both within the top quartile of enriched targets. Nanog broadly inhibits mESC differentiation, and its expression is reduced as cells lose pluripotency and commit to extraembryonic and somatic cell lineages in culture (29, 30). Klf2, along with Klf4 and Klf5, inhibits mesendoderm differentiation. Knockdown of Klf factors up-regulates primitive streak markers, as well as Cdx2, a gene expressed in trophectoderm and extraembryonic mesoderm (31). Also consistent with a role for Brf1 in promoting mesendoderm, the pluripotency factors Kdm4c ($E_{RIP} = 0.63$) and Zfp143 ($E_{RIP} = 0.99$) were enriched in the RIPseq assay. Knockdown of the lysine methyl-transferase Kdm4c is known to up-regulate mesendoderm and extraembryonic mesoderm markers (32). Zfp143 coordinates with Oct4 to transcriptionally activate Nanog. siRNA knockdown of Zfp143 rapidly initiates differentiation and promotes the expression of Fgf5, Cdx2, and Cdh3, which are expressed in trophectoderm and cells that commit to extraembryonic mesoderm (33). Understanding the regulation of these mRNAs may provide additional mechanistic insights into the Brf1-dependent control of gene expression in mESCs.

Brf1 Binds Nanog mRNA in Vitro. To corroborate these RIPseq results, we assayed for direct binding of Brf1 to an enriched mRNA, in this case, Nanog (Fig. 6*A*). Previous work has shown that Nanog is strongly regulated by FGF/Erk MAP kinase signaling (34), and these effects are mediated, in part, by direct regulation of the Nanog promoter (35). Posttranscriptional regulation by Brf1 would provide an alternative mechanism to repress Nanog expression.

We conducted a protein pull-down assay using RNA as bait (Fig. 6*B*, *Left*). Wild-type RNA and variants with ARE sequence mutations were expressed in vitro and hybridized at their 3′ ends to DNA oligonucleotides coupled to magnetic microbeads. These RNA–microbead conjugates were then incubated with crude cytoplasmic protein extracts, and all proteins capable of binding hybridized RNAs were magnetically isolated and purified for further analysis.

We used the 3′-UTR sequence of IL-2 as a positive control, because it contains clusters of ARE sequences that are bound and regulated by Zfp36 AUBPs (Fig. S2*A*) (36). Western blots showed that Brf1 could be purified from mESC lysates using a conjugated wild-type IL-2 sequence, but not using a mutant IL-2 lacking known AREs (Fig. 6*B*). Two Brf1 bands of different sizes were detected, possibly indicating the purification of different posttranslationally modified forms of Brf1 (Fig. 6*B*).

We next repeated the assay using Nanog mRNA as bait. The 3′-UTR of Nanog mRNA is ∼1 kb and contains three potential ARE elements: one full consensus (site 1 in Fig. 6*A*) and two partial nonconsensus sequences (sites 2 and 3 in Fig. 6*A*). Western blotting of these protein pull downs indicated that Brf1 bound to wild-type Nanog mRNA (Fig. 6*B*). Mutating the full-consensus ARE (site 1) significantly reduced Brf1 binding. Removing the remaining two partial nonconsensus AREs (sites 2 and 3) did not appear to further reduce the Brf1 signal. In contrast, the presence or absence of AREs did not affect the binding of other RNA-binding proteins (RBPs). For example, addition of an androgen receptor 3′-UTR sequence, which contains a poly(C) RNA-binding protein 1 (PCBP1) site, to Nanog mRNA permitted isolation of PCBP1 protein (Fig. S2*B*). This binding was not affected by the presence or absence of Nanog's AREs. In contrast, a Nanog mRNA containing only a 120-nt poly(A) without a PCBP1 site did not bind PCBP1 protein. Together, these results confirm that Brf1 binds specifically to Nanog mRNA in an ARE-dependent manner.

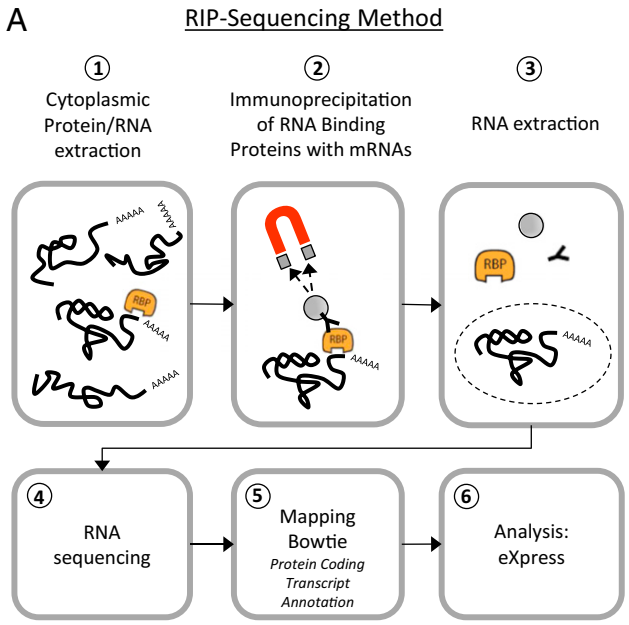

	Raw Sequencing Reads	Uniquely Mapped Reads
Total RNA 1	41,504,591	31,195,095
Total RNA 2	31,255,823	22,623,281
Brf1/2 RIP Sample 1	37,909,362	7,075,298
Brf1/2 RIP Sample 2	27,965,675	5,157,037
Rabbit IgG RIP Control 1	23,262,834	2,244,609
Rabbit IgG RIP Control 2	38,725,737	3,910,793

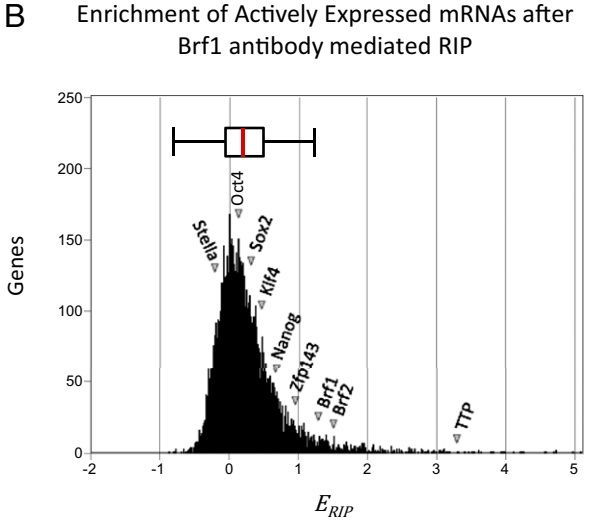

Percentile (x) of E_{RIP} Values	Full ARE	Partial ARE	genes
x ≥ 89 %tile (Positive Outliers)	25.1%	60.0%	418
x ≥ 75 %tile (Top Quartile)	13.8%	38.9%	1798
75 %tile ≥ x ≥ 25 %tile	5.8%	18.8%	3597
x ≤ 25 %tile (Bottom Quartile)	6.7%	20.5%	1799

Fig. 5. Brf1 binds other pluripotency-associated mRNAs. (*A*) Method used for RNA–RBP immunoprecipitation and RNA sequencing (RIPseq). Sequencing statistics for two total RNA samples, two Brf1/2 antibody RIP-derived samples, and two rabbit IgG RIP controls are presented. (*B*) Distribution of E_{RIP} values for actively expressed genes (n = 7,194 genes). The location of several notable pluripotency associated transcripts is highlighted. Box plot statistics: Median (red line, E_{RIP} = 0.17), lower quartile boundary (E_{RIP} = −0.04), upper quartile boundary (E_{RIP} = 0.47), and statistical outliers [median ± 1.5 × (upper quartile − lower quartile)]. Table: Frequency of full ARE motifs (-UUAUUUAUU-) and partial ARE motifs (-UAUUUAU-) among genes classified as E_{RIP} outliers or in different E_{RIP} quartiles.

FGF/Erk MAP Kinase Signaling Regulates Nanog mRNA Half-Life Through its AREs. To understand how Brf1 binding impacts Nanog expression, we measured the Nanog mRNA half-life, with or without AREs, and with or without FGF signaling, in *fgf4*$^{-/-}$ mESCs (Fig. 6*C*). We determined that the half-life of Nanog mRNA is 2.5 ± 0.4 h (±SEM) without FGF4/heparin and 1.5 ± 0.3 h (±SEM) with Fgf4/heparin (Fig. 6*C*, *Top*). However, removing all 3′-UTR ARE sites [ΔARE (1–3)] protected Nanog from increased degradation by FGF signaling (Fig. 6*C*, *Middle*), indicating that FGF destabilizes Nanog mRNA through its AREs. Additionally, when we analyzed H2B-YFP mRNA as a negative control, we observed no effect of FGF signaling on half-life (Fig. 6*C*, *Bottom*).

Unexpectedly, mutant Nanog mRNA [ΔARE (1–3)] exhibited a shorter half-life than wild type (2 h instead of 2.5 h; Fig. 6*C*). In the absence of FGF, we would have expected that the half-life of mutant and wild-type mRNAs to be the same. However, it is possible that Nanog's AREs are subject to regulation by other protein factors that have different effects. For example, AREs could associate with stabilizing AUBPs, such as HuR, whose activity is independent of FGF/Erk MAP kinase signaling in mESCs (Fig. 1*C*). Primary sequence changes may have also affected mRNA stability independent of any particular AUBP. Despite this difference, the above data clearly show that Nanog's AREs are necessary for any posttranscriptional regulation by FGF.

To show that FGF regulates Nanog through Brf1, we conducted an epistasis test in *fgf4*$^{-/-}$ R1 mESCs. We transfected mock or Brf1 siRNAs, and measured changes in Brf1 and Nanog mRNA level both in the presence and absence of FGF4/heparin. Relative to siRNA control (Fig. 6*D*, first column), Brf1 siRNAs caused a slight (~10%) down-regulation of Brf1 and a corresponding increase in Nanog mRNA levels (Fig. 6*D*, second column). These data indicate that Brf1 is expressed, albeit at a lower level, even when FGF signaling is absent (Fig. S2*C*) and that alternative pathways support its basal expression. We confirmed that FGF signaling remains the dominant regulator of Erk in mESCs (Fig. 2*D*) and that Erk MAP kinase signaling is the main driver of Brf1 expression (Fig. S2*C*).

Addition of FGF4/heparin ligand increased Brf1 and decreased Nanog by greater than twofold within 5 h (Fig. 6*D*, third column). In agreement with its role as a regulatory intermediate, the presence of Brf1 siRNAs reduced this regulation, yielding a smaller up-regulation of Brf1 and a smaller down-regulation of Nanog (Fig. 6*D*). We note that the inability of Brf1 siRNAs to fully block the down-regulation of Nanog can be partly explained by its limited knockdown efficiency (~75%) (Fig. 3*C*) but could also reflect Brf1-independent regulatory mechanisms.

FGF/Erk MAP kinase signaling thus regulates the dynamic expression of Zfp36 AUBPs in mESCs, which in turn affect the stability of key mRNA targets. In particular, we show that Brf1 (*zfp36l1*) has the capacity to broadly impact the regulation of core pluripotency-associated transcription factors, down-regulate self-renewal, and promote lineage-specific commitment during differentiation. In this way, Brf1 provides a specific molecular link between FGF/Erk MAP kinase signaling and the regulation of gene expression in mESCs.

Discussion

AUBPs modulate developmental gene expression in response to intercellular and intracellular signals. Some specific examples of this regulation include the repression of Notch1 in response to PI3K/Erk MAP kinase signals during T-cell development (17),

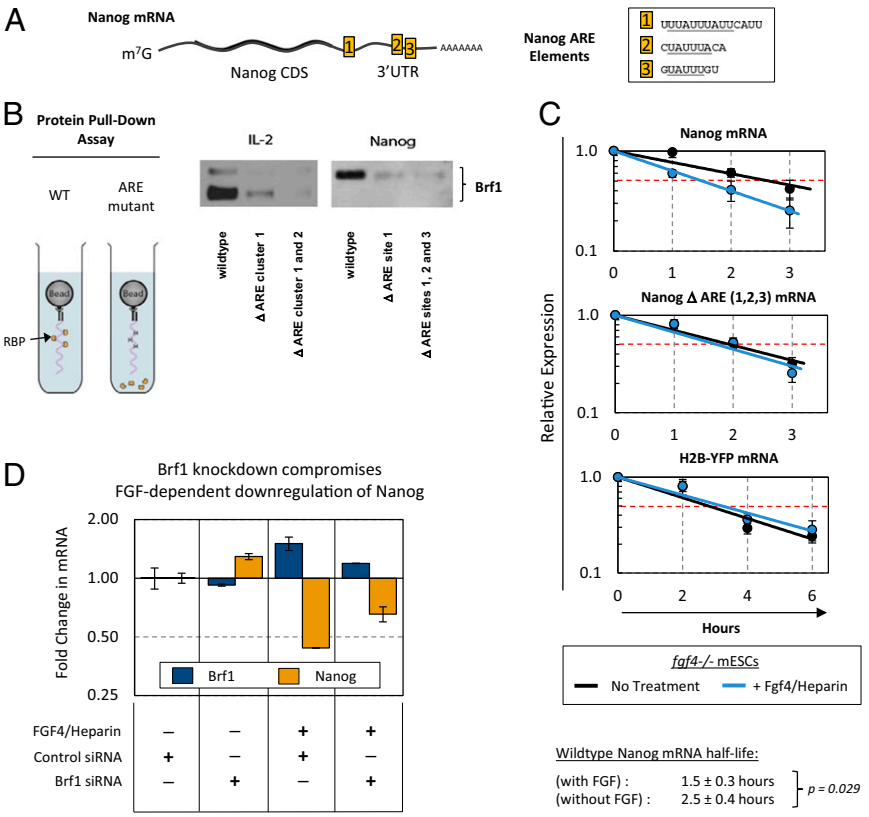

Fig. 6. Nanog is bound and regulated by Brf1. (*A*) Cartoon illustration of Nanog mRNA indicating the relative location and sequence of AREs in the 3′-UTR. ARE mutants were generated by changing the core (-ATTTA-) motif to (-AGGGA-). (*B*) (*Left*) Schematic diagram of the assay used to extract RBPs from crude protein extracts. Beads are conjugated to mRNAs with or without AREs. (*Right*) Western blot for Brf1 protein, present in IL-2 and Nanog mRNA protein isolates. ARE site mutations reduced the extraction of Brf1 from crude protein lysates for both IL-2 sequence control and Nanog mRNA. For more information on IL-2 sequence, see Fig. S2*A*. For more information on assay-specific controls, see Fig. S2*B*. (*C*) Changes in mRNA half-life were profiled in the presence (blue data points) or absence (black data points) of FGF signaling in *fgf4*$^{-/-}$ mESCs for wild-type Nanog mRNA (*Top*), mutant Nanog mRNA with deleted AREs [ΔARE (1–3)] (*Middle*), and H2B-YFP mRNA (*Bottom*) (±SEM; $n = 4$). The red dashed lines indicate one-half of the initial mRNA concentration. (*D*) Transfection of Brf1 siRNAs can compromise the regulation of Nanog by FGF4/heparin in *fgf4*$^{-/-}$ R1 mESCs (±SD; $n = 2$). See also Fig. S2*C*.

repression of TNF-α in response to p38/Erk MAP kinase signals during inflammation (37), and the stabilization of p21 in response to ATR/ATM kinase activation after DNA damage (38). Here, we demonstrate AUBPs mechanistically connect FGF/Erk MAP kinase signaling to the regulation of pluripotency, self-renewal, and differentiation in mESCs. More specifically, control over Brf1 expression rapidly regulates the expression of key pluripotency-associated genes, reduces the capacity to self-renew, and enhances mesendoderm differentiation upon LIF withdrawal.

Why has Brf1 been selected for implementing FGF-dependent cellular responses in mESCs? One possibility is that, owing to its rapid transcriptional response to FGF signaling and its short protein and mRNA half-life (~1.5 and ~1 h, respectively), Brf1 is capable of tracking dynamic changes in Erk MAP kinase activity. Brf1 directly affects mRNA abundance and provides stem cell populations with a mechanism to quickly respond to changes in FGF signaling, without necessarily altering underlying transcriptional states. However, the benefit of these dynamical properties to the biology of pluripotent or differentiating mESCs still remains unclear. Brf1 also provides a regulation that is similar to miRNAs, which also provide mRNA-level repression while maintaining flexibility in target selection. Interestingly, Zfp36 AUBPs and miRNAs are known to cooperate in regulating some mRNA targets (39), indicating a potential point of convergence between these two regulatory mechanisms. Future work will address why this system is particularly well adapted to serve as a regulator in mESCs, and as a mediator of FGF/Erk MAP kinase signaling.

Whether Brf1 plays a similar role in the embryo is unclear. We note that the regulatory effects of Brf1 in cell culture mimic the developmental response to FGF/Erk MAP kinase signaling at different stages of embryonic development. For example, FGF4 signaling promotes extraembryonic endoderm differentiation in the inner cell mass partly by destabilizing the expression of pluripotency genes (40). Brf1 may participate in this process by repressing Nanog and other pluripotency regulators. At a slightly later developmental stage, and one that is more relevant to mESCs, both FGF4 and FGF8 are required for mesoderm induction (41, 42). The expression of Brachyury, a regulator of mesoderm morphogenesis, is enhanced by FGF4 and FGF8 signaling through unknown mechanisms (43). Our results show that Brf1 expression during differentiation in mESCs similarly enhances Brachyury and other primitive streak markers. This regulatory connection could explain why Brf1 knockout mice also exhibit the same gross defects in chorio-allantoic fusion, neural tube closure, and placental organization at midgestation (E11) as FGFR2 knockouts, an indication of shared regulation and function (9, 44). Although the regulation of FGF/Erk MAP kinase signaling likely differs between the embryonic and cell culture context, these observations implicate Brf1 as an important FGF/Erk MAP kinase-inducible regulator of development in both systems.

Materials and Methods

RT-qPCR Experiments. Total RNA was harvested from samples and controls using Qiazol Reagent (Qiagen) or an RNeasy Mini Kit (Qiagen). RT of iso-

lated mRNA into cDNA was accomplished using iScript cDNA Synthesis Kit (Bio-Rad). A single qPCR reaction was composed of 0.5 μL of cDNA, primers or primers with probes, and qPCR reaction mix (diluted to a final volume of 10 μL). For qPCR experiments using TaqMan/hydrolysis probes (5′ dye: fluorescein amidite; 3′ quencher: Zen/Iowa Black FQ), cDNAs were profiled with SsoFast Probes Supermix Reagent (Bio-Rad) using the manufacturer-recommended protocol. In brief, we used a two-step thermocycling protocol (an initial 30-s 95 °C melt, followed by 40 cycles of 5-s 95 °C melt and 10-s 60 °C anneal/extend). For mRNA half-life qPCR experiments using primers only, cDNAs were profiled with SsoFast EvaGreen Supermix Reagent (Bio-Rad) using the manufacturer-recommended protocol. In brief, we used a two-step thermocycling protocol (initial 30-s 95 °C melt, followed by 40 cycles of 5-s 95 °C melt and 10-s 55 °C anneal/extend), terminating with a postamplification melt curve analysis (initialized at 60 °C, and increased at 0.5 °C increments every 10 s to 95 °C). All measurements were made using a Bio-Rad CFX96 Real-Time PCR System (Bio-Rad). See primer and probe characterization (Table S2).

Cell Lines and Cell Culture. *fgf4*$^{-/-}$ mESCs (strain FD6) were a kind gift from Dr. Angie Rizzino (University of Nebraska Medical Center, Omaha, NE).

Cultures were routinely passaged in complete ES culture medium [15% (vol/vol) FBS, 1,000 U/mL LIF, nonessential amino acid (NEAA), sodium pyruvate, and β-mercaptoethanol (βME) in DMEM] in the absence of feeders. Mesoderm differentiation media contained the following: 15% (vol/vol) FBS, NEAA, sodium pyruvate, and βME in DMEM (23); neurectodermal differentiation media contained the following: N2B27 serum free media (45).

Reagents, Antibodies, Signaling Inhibitors, and siRNAs. Reagents included the following: Qiazol reagent (Qiagen); iScript Kit (Bio-Rad); SsoFast Probes Supermix (Bio-Rad).

Antibodies included the following: mouse monoclonal (L34F12) anti-p44/p42 (Cell Signal; catalog #4696; 1:2,000); rabbit monoclonal (D13.14.4E) anti-phospho-p44/p42 (Cell Signal; catalog #4370; 1:2,000); mouse anti-TBP (Abcam; catalog #ab818; 1:1,000); rabbit anti–β-Tubulin (Abcam; catalog #ab6046; 1:1,000); rabbit polyclonal anti-Brf1/2 (Cell Signal; catalog #2119; 1:1,000); rabbit anti-Zfp36 (Protein Tech Group; catalog #12737-1-AP; 1:500); rabbit anti-hnRNP E1 (Cell Signal; catalog #8534; 1:500); goat anti-Brachyury (R&D Systems; catalog #AF2085; 1:200); rabbit anti-Sox1 (GeneTex; catalog #GTX62974; 1:200); mouse anti-Gapdh (Abcam; catalog #ab8245; 1:5,000).

Signaling inhibitors included the following: CI-1040 (also known as PD184352; Axon; 5 μM); PD173074 (Sigma; 100 ng/mL).

siRNAs included the following: TTP siRNA (Santa Cruz Biotechnology; 10 nM); Brf1 siRNA (Santa Cruz Biotechnology; 10 nM); Brf2 siRNA (Santa Cruz Biotechnology; 10 nM); All Stars Negative Control siRNA (Qiagen; 10 nM).

Measurement of mRNA Half-Life. mESC cultures were cotransfected with a reverse Tet (rTet) expression plasmid (PGK-H2B-mCherry/T2A/rTet) and either CMV(2xTetO)-H2B-YFP or CMV(2xTetO)-Nanog with and without ARE site mutations at 19:1 ratio by mass. Culture media was then transitioned to media containing FGF4 and heparin (10 ng/mL and 10 μg/mL, respectively) or PBS to determine the regulatory effect of ERK MAP kinase signaling in *fgf4*$^{-/-}$ *cells*. To stop transcription from the CMV-TO promoter, doxycycline was added to a concentration of 1 μg/mL to permit binding of rTet to TetO sequences. Changes in the abundance of H2B-YFP or Nanog mRNA relative to Gapdh, Sdha, and Tbp housekeeping genes was measured using RT-qPCR. To distinguish from endogenous Nanog mRNA, we developed a primer set that specifically recognizes the 5′-UTR of Nanog expressed from the CMV(2×TetO) promoter.

Isolation of RBPs from Crude Cytoplasmic Lysates. IL-2 and Nanog RNAs were produced in vitro using T7 Ampliscribe (Epicentre Technologies). These RNAs were then hybridized to biotin-DNA oligonucleotides at their 3′ end. Two hundred picomoles of IL-2 or Nanog RNA were used for 250 pmol of biotin-DNA oligonucleotide. Hybridization reactions were added to 1 mg of streptavidin magnetic agarose beads (New England Biolabs). Crude cytoplasmic extracts used for protein pull-down assays were obtained using NE-PER reagents (Thermo Scientific). RNA/DNA–bead conjugates were incubated in crude cytoplasmic extract for 1 h at 4 °C, washed five times with Binding Buffer (20 mM Tris·HCl, pH 7.5, 50 mM KCl, 1 mM EDTA, 1 mM DTT, 0.5% Triton X-100 with RNase inhibitors) and incubated in High Salt Elution Buffer (Binding Buffer plus 1 M NaCl) to collect RNA-bound protein fractions. Protein pull downs were analyzed via Western blot.

Preparation of Cells for Flow Cytometry. Cultures were harvested with 0.25% trypsin-EDTA, dispersed into a cell suspension, and added to an equal volume of 4% formaldehyde. Cells were fixed for 5 min, quenched, and gently pelleted at 500 × *g* for 30 s. Supernatants were removed and cell pellets were resuspended in 2.5 mg/mL BSA in 1× HBSS. The resulting cell suspensions were incubated overnight at 4 °C before flow cytometry analysis. For antibody-stained cell suspensions, cell pellets containing fixed cells were resuspended in 10% FBS in PBS to block, gently pelleted, and stained with appropriate primary and secondary antibodies at 4 °C. Before flow cytometry analysis, cells were pelleted and resuspended in 2.5 mg/mL BSA in 1× HBSS. All samples, stained and unstained, were analyzed with a Miltenyi Biotec VYB flow cytometer. Compensation and background correction were applied postacquisition.

RNA/RBP Immunoprecipitation and RNA Sequencing. RBP–mRNA complexes were isolated using a Magna-RIP kit (Millipore). Briefly, cytoplasmic extract from ∼1 × 10^7 E14 mESCs was distributed equally among two samples and two controls. For sample reactions, 5 μg of α-Brf1/2 antibody was used for 50 μL of magnetic protein A/G beads. For control reactions, 5 μg of rabbit IgG with no immunoreactivity was used for 50 μL of magnetic protein A/G beads. After stringency washes and proteinase K digestion, RNA was isolated using Qiazol reagent.

RNA/RBP immunoprecipitation (RIP)-purified RNAs and total RNA from E14 mESCs were prepared for sequencing using a TruSeq RNA Sample Prep kit. RNAs were fragmented to generate lengths of ∼200 nt, reverse transcribed with random hexameric primers to generate double-stranded DNA, blunted, adenylated, and ligated to Illumina sequencing adapters (150 bp). DNA fragments were gel separated, and all fragments running at 350 bp were extracted and amplified. Amplified DNA fragments were then sequenced using an Illumina HiSeq2000.

RNA-Sequencing Analysis Tools and Methods. Raw sequencing reads were trimmed (of 13 nt from 5′ end) before Bowtie mapping using a mouse transcript annotation containing only protein coding genes (18,313 genes), derived from NCBI37/mm9 genome build. Mapping statistics were generated using eXpress (46). For enrichment analysis, fragments per kilobase exon per million mapped reads (FPKM) were used as a measure of transcript abundance (47).

We computed a statistic ($E_{RIP,n}$) that represents the degree to which the abundance of the *n*th transcript is enriched by antibody-mediated RIP. This statistic uses differences in a transcript's abundance after Brf1/2 antibody RIP (mean $\text{FPKM}_{\text{BRF},n}$) compared with rabbit IgG RIP (mean $\text{FPKM}_{\text{IgG},n}$), normalized by their initial abundance in total RNA before RIP (mean $\text{FPKM}_{\text{Total},n}$). This difference was further normalized by a penalty factor (P), which accounts for a transcript's tendency to be nonspecifically purified, and is thus a saturating function of transcript abundance in the IgG control experiment:

$$E_{RIP,n} = \frac{\left(A_{BRF,n} - A_{IgG,n}\right)}{P},$$

where

$$A_{BRF,n} = \frac{\text{mean FPKM}_{\text{BRF},n}}{\text{mean FPKM}_{\text{Total},n}},$$

$$A_{IgG,n} = \frac{\text{mean FPKM}_{\text{IgG},n}}{\text{mean FPKM}_{\text{Total},n}},$$

$$P = \text{median}\left(A_{IgG}\right) + A_{IgG,n}.$$

Although $A_{IgG,n}$ captures the level of nonspecific association of a transcript with assay components (i.e., protein A/G beads, rabbit IgG, etc.), nonspecific association of transcripts with immunoprecipitated RBP/RNA complexes could not be independently quantified, and could contribute a background to these $E_{RIP,n}$ values.

High-Throughput Sequencing Data. Raw sequencing data discussed in this publication were deposited in the National Center for Biotechnology Information Gene Expression Omnibus database (accession no. GSE40104).

ACKNOWLEDGMENTS. We thank Dr. Kathrin Plath (University of California, Los Angeles) and Dr. Angie Rizzino (University of Nebraska Medical Center) for the kind donation of cell culture reagents; Dr. Azim Surani (University of Cambridge) for fruitful discussions; Rochelle Diamond, Diana Perez, and Josh Verceles from the Caltech Flow Cytometry Facility; Igor Antoshechkin and Vijaya Kumar from the Millard and Muriel Jacobs Genetics and Genomics Laboratory at Caltech; Leah Santat, Yaron Antebi, Joe Markson, James

Linton, Pierre Neveu, John Yong, Zakary Singer, Julia Tischler, Joe Levine, and Sandy Nandagopal for fruitful discussions. This work was supported by a Human Frontiers Science Program Grant (RGP0020/2012), the Weston Havens Foundation, and the David and Lucille Packard Foundation. F.E.T. was supported by the National Defense Science and Engineering Graduate Research Fellowship.

1. Colegrove-Otero LJ, Minshall N, Standart N (2005) RNA-binding proteins in early development. *Crit Rev Biochem Mol Biol* 40(1):21–73.
2. Kwon SC, et al. (2013) The RNA-binding protein repertoire of embryonic stem cells. *Nat Struct Mol Biol* 20(9):1122–1130.
3. Glisovic T, Bachorik JL, Yong J, Dreyfuss G (2008) RNA-binding proteins and post-transcriptional gene regulation. *FEBS Lett* 582(14):1977–1986.
4. Okano HJ, Darnell RB (1997) A hierarchy of Hu RNA binding proteins in developing and adult neurons. *J Neurosci* 17(9):3024–3037.
5. Baou M, Norton JD, Murphy JJ (2011) AU-rich RNA binding proteins in hematopoiesis and leukemogenesis. *Blood* 118(22):5732–5740.
6. Wiszniak SE, Dredge BK, Jensen KB (2011) HuB (elavl2) mRNA is restricted to the germ cells by post-transcriptional mechanisms including stabilisation of the message by DAZL. *PLoS One* 6(6):e20773.
7. Chi MN, et al. (2011) The RNA-binding protein ELAVL1/HuR is essential for mouse spermatogenesis, acting both at meiotic and postmeiotic stages. *Mol Biol Cell* 22(16): 2875–2885.
8. Katsanou V, et al. (2009) The RNA-binding protein Elavl1/HuR is essential for placental branching morphogenesis and embryonic development. *Mol Cell Biol* 29(10):2762–2776.
9. Stumpo DJ, et al. (2004) Chorioallantoic fusion defects and embryonic lethality resulting from disruption of Zfp36L1, a gene encoding a CCCH tandem zinc finger protein of the Tristetraprolin family. *Mol Cell Biol* 24(14):6445–6455.
10. Bourcier C, et al. (2011) Constitutive ERK activity induces downregulation of tristetraprolin, a major protein controlling interleukin8/CXCL8 mRNA stability in melanoma cells. *Am J Physiol Cell Physiol* 301(3):C609–C618.
11. Amit I, et al. (2007) A module of negative feedback regulators defines growth factor signaling. *Nat Genet* 39(4):503–512.
12. Lanner F, Rossant J (2010) The role of FGF/Erk signaling in pluripotent cells. *Development* 137(20):3351–3360.
13. Nichols J, Smith A (2011) The origin and identity of embryonic stem cells. *Development* 138(1):3–8.
14. Hamazaki T, Kehoe SM, Nakano T, Terada N (2006) The Grb2/Mek pathway represses Nanog in murine embryonic stem cells. *Mol Cell Biol* 26(20):7539–7549.
15. Ying QL, et al. (2008) The ground state of embryonic stem cell self-renewal. *Nature* 453(7194):519–523.
16. Dailey L, Ambrosetti D, Mansukhani A, Basilico C (2005) Mechanisms underlying differential responses to FGF signaling. *Cytokine Growth Factor Rev* 16(2):233–247.
17. Hodson DJ, et al. (2010) Deletion of the RNA-binding proteins ZFP36L1 and ZFP36L2 leads to perturbed thymic development and T lymphoblastic leukemia. *Nat Immunol* 11(8):717–724.
18. Lu JY, Schneider RJ (2004) Tissue distribution of AU-rich mRNA-binding proteins involved in regulation of mRNA decay. *J Biol Chem* 279(13):12974–12979.
19. Doller A, Pfeilschifter J, Eberhardt W (2008) Signalling pathways regulating nucleocytoplasmic shuttling of the mRNA-binding protein HuR. *Cell Signal* 20(12):2165–2173.
20. Barreau C, Paillard L, Osborne HB (2005) AU-rich elements and associated factors: Are there unifying principles? *Nucleic Acids Res* 33(22):7138–7150.
21. Wilder PJ, et al. (1997) Inactivation of the FGF-4 gene in embryonic stem cells alters the growth and/or the survival of their early differentiated progeny. *Dev Biol* 192(2): 614–629.
22. Ivanova N, et al. (2006) Dissecting self-renewal in stem cells with RNA interference. *Nature* 442(7102):533–538.
23. Nishikawa SI, Nishikawa S, Hirashima M, Matsuyoshi N, Kodama H (1998) Progressive lineage analysis by cell sorting and culture identifies FLK1+VE-cadherin+ cells at a diverging point of endothelial and hemopoietic lineages. *Development* 125(9): 1747–1757.
24. Ying QL, Nichols J, Chambers I, Smith A (2003) BMP induction of Id proteins suppresses differentiation and sustains embryonic stem cell self-renewal in collaboration with STAT3. *Cell* 115(3):281–292.
25. Keene JD, Komisarow JM, Friedersdorf MB (2006) RIP-Chip: The isolation and identification of mRNAs, microRNAs and protein components of ribonucleoprotein complexes from cell extracts. *Nat Protoc* 1(1):302–307.
26. Lai WS, Parker JS, Grissom SF, Stumpo DJ, Blackshear PJ (2006) Novel mRNA targets for tristetraprolin (TTP) identified by global analysis of stabilized transcripts in TTP-deficient fibroblasts. *Mol Cell Biol* 26(24):9196–9208.
27. Tchen CR, Brook M, Saklatvala J, Clark AR (2004) The stability of tristetraprolin mRNA is regulated by mitogen-activated protein kinase p38 and by tristetraprolin itself. *J Biol Chem* 279(31):32393–32400.
28. Sarkar B, Xi Q, He C, Schneider RJ (2003) Selective degradation of AU-rich mRNAs promoted by the p37 AUF1 protein isoform. *Mol Cell Biol* 23(18):6685–6693.
29. Chambers I, et al. (2003) Functional expression cloning of Nanog, a pluripotency sustaining factor in embryonic stem cells. *Cell* 113(5):643–655.
30. Mitsui K, et al. (2003) The homeoprotein Nanog is required for maintenance of pluripotency in mouse epiblast and ES cells. *Cell* 113(5):631–642.
31. Jiang J, et al. (2008) A core Klf circuitry regulates self-renewal of embryonic stem cells. *Nat Cell Biol* 10(3):353–360.
32. Loh YH, Zhang W, Chen X, George J, Ng HH (2007) Jmjd1a and Jmjd2c histone H3 Lys 9 demethylases regulate self-renewal in embryonic stem cells. *Genes Dev* 21(20): 2545–2557.
33. Chen X, Fang F, Liou YC, Ng HH (2008) Zfp143 regulates Nanog through modulation of Oct4 binding. *Stem Cells* 26(11):2759–2767.
34. Chazaud C, Yamanaka Y, Pawson T, Rossant J (2006) Early lineage segregation between epiblast and primitive endoderm in mouse blastocysts through the Grb2-MAPK pathway. *Dev Cell* 10(5):615–624.
35. Santostefano KE, Hamazaki T, Pardo CE, Kladde MP, Terada N (2012) Fibroblast growth factor receptor 2 homodimerization rapidly reduces transcription of the pluripotency gene Nanog without dissociation of activating transcription factors. *J Biol Chem* 287(36):30507–30517.
36. Ogilvie RL, et al. (2005) Tristetraprolin down-regulates IL-2 gene expression through AU-rich element-mediated mRNA decay. *J Immunol* 174(2):953–961.
37. Deleault KM, Skinner SJ, Brooks SA (2008) Tristetraprolin regulates TNF TNF-alpha mRNA stability via a proteasome dependent mechanism involving the combined action of the ERK and p38 pathways. *Mol Immunol* 45(1):13–24.
38. Wang W, et al. (2000) HuR regulates p21 mRNA stabilization by UV light. *Mol Cell Biol* 20(3):760–769.
39. Jing Q, et al. (2005) Involvement of microRNA in AU-rich element-mediated mRNA instability. *Cell* 120(5):623–634.
40. Frankenberg S, et al. (2011) Primitive endoderm differentiates via a three-step mechanism involving Nanog and RTK signaling. *Dev Cell* 21(6):1005–1013.
41. Boulet AM, Capecchi MR (2012) Signaling by FGF4 and FGF8 is required for axial elongation of the mouse embryo. *Dev Biol* 371(2):235–245.
42. Sun X, Meyers EN, Lewandoski M, Martin GR (1999) Targeted disruption of Fgf8 causes failure of cell migration in the gastrulating mouse embryo. *Genes Dev* 13(14): 1834–1846.
43. Schulte-Merker S, Smith JC (1995) Mesoderm formation in response to Brachyury requires FGF signalling. *Curr Biol* 5(1):62–67.
44. Xu X, et al. (1998) Fibroblast growth factor receptor 2 (FGFR2)-mediated reciprocal regulation loop between FGF8 and FGF10 is essential for limb induction. *Development* 125(4):753–765.
45. Ying QL, Stavridis M, Griffiths D, Li M, Smith A (2003) Conversion of embryonic stem cells into neuroectodermal precursors in adherent monoculture. *Nat Biotechnol* 21(2):183–186.
46. Roberts A, Pachter L (2013) Streaming fragment assignment for real-time analysis of sequencing experiments. *Nat Methods* 10(1):71–73.
47. Trapnell C, et al. (2010) Transcript assembly and quantification by RNA-Seq reveals unannotated transcripts and isoform switching during cell differentiation. *Nat Biotechnol* 28(5):511–515.